

Bound excitons and resonant Raman scattering in $\text{Cd}_x\text{Zn}_{1-x}\text{Te}$ ($0.9 \leq x \leq 1$)

E. Cohen* and R. A. Street

Xerox Palo Alto Research Center, 3333 Coyote Hill Road, Palo Alto, California 94304

A. Muranevich

Solid State Institute, Technion, Haifa 32000, Israel

(Received 1 August 1983)

Luminescence and resonant LO-phonon Raman scattering spectra of CdTe, $\text{Cd}_{0.97}\text{Zn}_{0.03}\text{Te}$, and $\text{Cd}_{0.9}\text{Zn}_{0.1}\text{Te}$ have been studied using selective, cw excitation in the temperature range of 1.7–100 K. The main spectral features are due to free excitons (polaritons), excitons bound to neutral donors (D^0, X), excitons bound to neutral acceptors (A^0, X) and a shallow bound-exciton band of unidentified origin (S band). In CdTe, the fine-structure components of the (A^0, X) 1S exciton have strongly temperature-dependent Lorentzian line shapes which are shown to be due to the interaction with acoustic phonons. The fine-structure components of the (D^0, X) 1S exciton have Gaussian line shapes, reflecting random electric fields acting on the bound exciton. In the mixed semiconductors, all lines are Gaussian because of the random potential fluctuations. Two thermally activated processes are found to quench exciton luminescence: (a) thermalization of the (A^0, X) exciton into the free-exciton band; (b) dissociation of the exciton into free carriers. The latter is found to be operative in (A^0, X), free-exciton, and S -band luminescence quenching. Strong resonance enhancement of LO-phonon Raman scattering is observed mainly in the (A^0, X) band. The cross-section spectrum is well explained by an homogeneous line broadening in CdTe and by an inhomogeneous one in $\text{Cd}_x\text{Zn}_{1-x}\text{Te}$. The intensity of the Raman lines is strongly temperature dependent, reflecting exciton-damping processes. Spectral diffusion is observed under selective excitation within the (A^0, X) band in the mixed crystals. However, it is attributed to exciton transfer within the states of the S band [which overlaps the (A^0, X) band] and not within the (A^0, X) band itself.

I. INTRODUCTION

Excitons in alloy semiconductors of the type $A_xB_{1-x}C$ are subjected to potential fluctuations which are set up by microscopic composition fluctuations.¹ These potential fluctuations introduce a low-energy tail of intrinsic excitons^{2,3} and an inhomogeneous broadening of bound-exciton lines^{4,5} [e.g., excitons bound to neutral donors (D^0, X), to neutral acceptors (A^0, X), or to isoelectronic traps]. Recently, several studies on exciton dynamics in $A_xB_{1-x}C$ -type semiconductors were reported.^{6–8} As in the case of binary semiconductors, thermally activated processes into extended states are observed. These include thermalization into the free-exciton band and exciton dissociation. In addition, exciton transfer between localized states has been identified both in the tail of intrinsic excitons^{9–11} and in an impurity-bound-exciton band.¹²

The important role which excitons play as intermediate states in resonant Raman scattering (RRS) is well known.¹³ The most detailed studies dealt with polariton bands derived from the 1S level of free excitons in direct-gap binary semiconductors.¹⁴ The effects of polariton dynamics on the RRS have not been studied in detail.¹⁵ RRS in alloy semiconductors was investigated with above-gap excitation.¹⁶ Klochikhin *et al.*¹⁷ have studied the temperature dependence of the RRS intensity in $\text{Cd}_x\text{Zn}_{1-x}\text{Te}$ ($x \sim 0.5$) and interpreted it in terms of exci-

ton damping by LO-phonon scattering, in addition to a temperature-independent exciton scattering by potential fluctuations. Fujii *et al.*¹⁸ reported a similar study in indirect-gap $\text{AgBr}_{1-x}\text{Cl}_x$ near the lowest-energy intrinsic exciton band. In this case, exciton damping is found to be due to trapping, intervalley scattering by zone-edge phonons, and intravalley scattering by acoustic phonons.

In this work the damping processes of excitons bound to neutral donors and acceptors in $\text{Cd}_x\text{Zn}_{1-x}\text{Te}$ ($0.9 \leq x \leq 1$) are studied by luminescence and LO-phonon RRS. A comparison between the alloyed crystals and CdTe shows that the effect of potential fluctuations on bound-exciton dynamics is negligible (in spite of the pronounced inhomogeneous line broadening). The (A^0, X) excitons couple strongly to piezoelectric phonons (both acoustic and optic). This is manifested by a strong LO-phonon sideband in luminescence, an enhanced LO-phonon RRS, and by the temperature dependence of the linewidth (in CdTe), luminescence, and RRS intensities. Nonradiative processes such as bound-exciton thermalization into the free-exciton band and exciton dissociation can be identified in the temperature dependence of the luminescence and RRS.

After describing the experimental procedures in Sec. II, we present the experimental results and model fitting in Sec. III. Since CdTe serves as a model system for bound excitons, their dynamics in this material are analyzed

first. Then the $\text{Cd}_x\text{Zn}_{1-x}\text{Te}$ alloy semiconductors are treated. A summary of this work as compared to the $\text{CdS}_x\text{Se}_{1-x}$ alloy semiconductors is given in Sec. IV.

II. EXPERIMENTAL PROCEDURES

Single crystals of CdTe and $\text{Cd}_x\text{Zn}_{1-x}\text{Te}$ ($x=0.02, 0.03, \text{ and } 0.1$) were grown from the melt by the modified Bridgman method under an overpressure of Cd.¹⁹ The samples used in this study had cleaved (110) faces. The exact composition (x) of the alloys was determined from the energy of the intrinsic exciton observed by luminescence at 2 K (see below). All crystals were n type with a room-temperature resistivity of $10^6 \Omega \text{ cm}$ (for $\text{Cd}_x\text{Zn}_{1-x}\text{Te}$) and $10^8 \Omega \text{ cm}$ (for CdTe).

While useful Ohmic contact could not be made on the crystals used in this study, other crystals with resistivity of $\sim 1 \Omega \text{ cm}$ were found to have 8×10^{15} carriers/cm³ at room temperature. We thus estimate that the impurity level in our samples was lower than this.

The crystals were placed in a variable-temperature Dewar and were immersed in either liquid-He or cold He gas. In the latter case, the temperature was stabilized within $\pm 0.3 \text{ K}$ over the range 4.4–100 K.

The excitation source for luminescence and Raman scattering was a tunable cw dye laser pumped by a Kr^+ laser. The power impinging on the sample ranged from 0.5–30 mW with the laser beam focused down to about a 1-mm² spot. The dye-laser linewidth was 0.3 Å (about 0.06 meV in the spectral range where the crystals radiate). The light emitted by the crystals was monitored with a

double monochromator (resolution of 0.2 Å) and processed with a photon-counting system.

III. RESULTS AND MODEL

A. CdTe

1. Exciton levels

This system serves as a model for the analysis of exciton spectra in the alloy semiconductors and was thus studied in some detail. Figure 1 shows photoluminescence spectra of CdTe excited at the polariton band and observed at three temperatures. The spectrum shown in Fig. 1(a), taken at 1.7 K, is similar to those reported by others^{20,21} for high-purity materials. The spectral components are identified as lines due to excitons bound to donors and acceptors and their LO-phonon sidebands. Also observed is the LO-phonon sideband of the polariton band and the two-electron transitions associated with (D^0, X) .^{22,23}

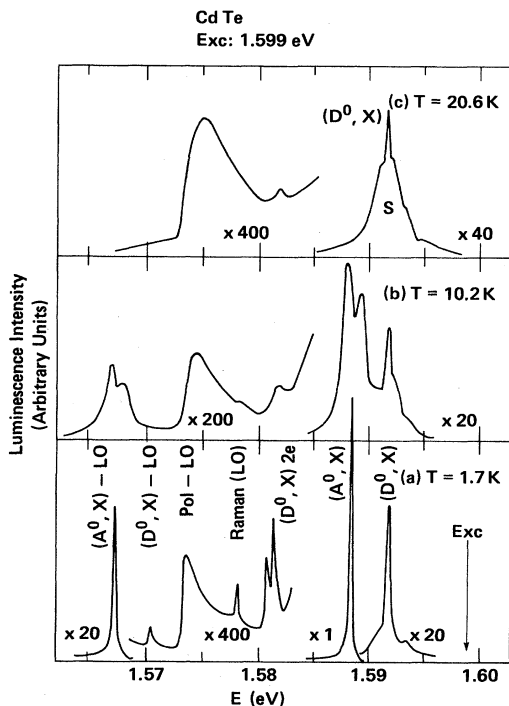


FIG. 1. Photoluminescence spectra of CdTe excited into the 1S polariton band. Gain used in each section is relative to that of the strongest feature, (A^0, X) at 1.7 K.

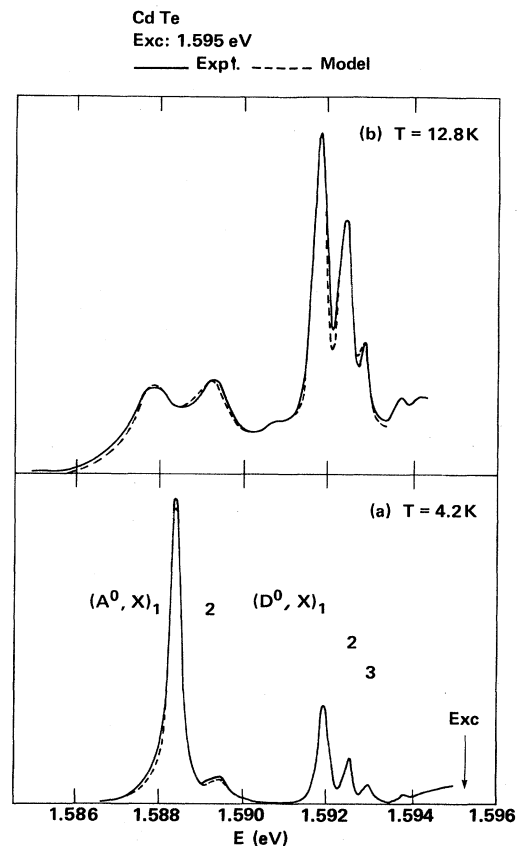


FIG. 2. Fine structure of the (D^0, X) and (A^0, X) 1S exciton in CdTe. Excitation is at the 1S polariton threshold. (A^0, X) lines are fitted with temperature-dependent Lorentzian line shapes. (D^0, X) lines are Gaussians convoluted with a narrower, temperature-dependent Lorentzian. Parameters used to fit the experimental spectra are given in the text. [In (a) the calculated curve coincides with the experimental data in the (D^0, X) spectral region.] Change in the relative intensity within each exciton complex reflects increased population of the higher levels.

Both (A^0, X) and (D^0, X) show a fine structure which can be seen in the high-resolution spectra of Fig. 2. This structure results from coupling between the spins of the three particles which form these exciton complexes.^{24,25} For the (A^0, X) bound exciton, three lines are expected (corresponding to the $J = \frac{5}{2}, \frac{3}{2},$ and $\frac{1}{2}$ states). By analogy to GaAs and InP,²⁶ the $J = \frac{1}{2}$ state is too weak to be observed. The identity of the acceptor giving rise to the two observed lines is unknown. It should be noted that Ag and Cu acceptors in CdTe yield a (A^0, X) line which corresponds to the $J = \frac{1}{2}$ state.²⁷ The binding energy of the acceptor- and donor-bound excitons are determined by measuring the energy separation of the LO-phonon sideband of the lowest component [$(A^0, X)_1$ -LO and $(D^0, X)_1$ -LO] from the cutoff of the polariton LO-phonon sideband. These energies are given in Table I.

For $T \geq 10$ K the luminescence spectra show that the (D^0, X) lines ride on a broad band [designated S in Fig. 1(c)]. In the temperature range of 20–80 K this is the strongest spectral feature. It could be argued that this band (or part of it) is an acoustic-phonon sideband of the $1S$ polariton. However, the excitation spectra of $(A^0, X)_1$ and $(D^0, X)_1$ taken at 1.7 K (Fig. 3) confirm the existence of an independent band. The $(D^0, X)_1$ excitation spectrum [Fig. 3(b)] reveals a series of excited states²⁰ in the narrow region of 1.593–1.595 eV. The two lowest-energy lines are $(D^0, X)_2$ and $(D^0, X)_3$. These lines ride on a broad background at the same energy range of the S band. The excitation spectrum also shows the $1S$ polariton band (low-energy threshold at 1.5955 eV). Its shape is similar to that of the LO-phonon sideband observed in luminescence [Fig. 1(a)]. The shape of the polariton band results from a nonthermalized distribution. The lifetime is probably too short to allow thermalization. The band designated $(D^0, X)^*$ has a threshold 7.5 meV above (D^0, X) and may derive from the $2S$ state of the exciton bound to the neutral donor. Figure 3(a) shows the excitation spectrum of the $(A^0, X)_1$ line. An excited state which was designated $(A^0, X)_2$ in Fig. 2 is observed 1.2 meV above the emitting line. This state is thermally populated at temperatures above 4 K. The S band is clearly observed as a strong region of excitation of $(A^0, X)_1$. Two free-exciton (polariton) bands, $1S$ and $2S$, are observed as well as a strong band designated $(A^0, X)^*$. Again, as this band has a threshold around 7 meV above (A^0, X) , it may derive from excited nS states of the exciton bound to the neutral acceptor.

TABLE I. Measured parameters of free and bound excitons in CdTe.

Exciton	Binding energy E_B (meV)	Activation energy (meV)	LO-phonon interaction (relative)
Polariton $1S$		$E_f = 12 \pm 1$	0.2
S band	~ 1.5	$E_f = 12 \pm 1$	$< 10^{-2}$
(D^0, X)	2.4		6×10^{-3}
(A^0, X)	5.7	$E_a = 6 \pm 1$	7×10^{-2}
		$E_f = 14 \pm 1$	

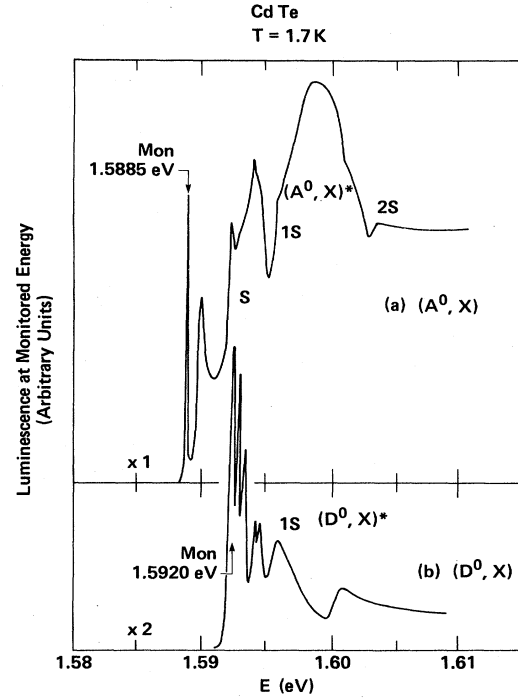


FIG. 3. Excitation spectra of (a) lowest component of the (A^0, X) $1S$ exciton and (b) lowest component of the (D^0, X) $1S$ exciton in CdTe.

The effects discussed later in this work (exciton linewidths and RRS) depend on the exciton-phonon interaction. A measure of the relative interaction strength between the various excitons and LO phonons can be obtained from the intensities of multiple phonon sidebands. By using the relation $I_n = I_0 \alpha^2 / n!$, where I_0 is the no-phonon-line intensity, α is the exciton-LO-phonon interaction strength, and n is the number of emitted phonons, the values obtained for α are listed in Table I. For the shallow S band, it is difficult to accurately determine this ratio because its LO-phonon sideband overlaps the LO plus acoustic-phonon sideband of the $1S$ polariton. Thus, only an upper limit of 10^{-2} can be obtained.

2. Temperature dependence

The thermally activated processes which affect bound-exciton emission intensity and linewidth are (a) relaxation between closely spaced levels, and (b) dissociation of the exciton or its thermalization into extended exciton states. In order to study these processes, a series of luminescence spectra were taken in the temperature range 2–70 K. For each spectrum the excitation energy and intensity were kept constant. Examples are the high-resolution spectra shown in Fig. 2, in which the no-phonon (A^0, X) and (D^0, X) lines are excited just below the polariton band. Consider first the group of three (D^0, X) lines centered near 1.5925 eV. The excitation spectrum [Fig. 3(b)] indicates that these lines arise from radiative recombination of the same donor species.²² From the relative intensities at various temperatures (Fig. 2) it is clear that these states do

not fully thermalize. The reason for this may be the weak exciton-phonon interaction of the (D^0, X) complex. In the temperature range of 2–15 K the line shape of the three (D^0, X) components can be fitted by three Gaussians, each convoluted with a Lorentzian (Voigt line shape),

$$f(E) = \sum_{i=1}^3 \int g_i(E-x)l(x)dx. \quad (1)$$

The calculated line shapes are shown by dashed lines in Fig. 2. The Gaussian full widths at half-maximum (FWHM) for the three (D^0, X) lines are 0.20, 0.25, and 0.28 (± 0.02) meV for the lines at 1.5930, 1.5926, and 1.5920, respectively. The Gaussian line shapes reflect the random distribution of potential fluctuations around the neutral donors to which the exciton binds. Presumably they are due to a distribution of charged donors and acceptors, and the broadening mechanism is similar to that proposed for shallow donor spectra.^{28,29} It should be noted that the linewidth decreases with decreasing binding energy. This means that the potential fluctuations average out for the less-bound states, whose wave functions is more spread out than that of the deepest $(D^0, X)_1$ state.

The additional Lorentzian broadening is due to the interaction of individual donor-bound excitons with acoustic phonons. Its FWHM is 0.05 ± 0.02 meV at 4.2 K and 0.1 ± 0.02 meV at 12.8 K for all (D^0, X) components. The Gaussian linewidths are temperature independent up to about 20 K. [Above this temperature it is difficult to fit the line shapes as the strong S -band emission masks the (D^0, X) lines.] As the inhomogeneous contribution to the linewidths is larger than the homogeneous contribution, the exact temperature dependence of the latter is difficult to determine. The small homogeneous broadening of the (D^0, X) lines is a result of the weak interaction with acoustic phonons. This is consistent with the fact that the (D^0, X) components do not fully thermalize.

The temperature dependence of the two (A^0, X) components is quite different. From 4.2 to about 16 K (at which they are too weak to be measured), they can be fitted with two Lorentzians whose widths are strongly temperature dependent. Figures 2(a) and 2(b) show the fit to the experimental results. Figure 4(a) gives the measured linewidths as a function of temperature. The homogeneous line shape and its temperature dependence result from the exciton-acoustic-phonon interaction. The theory has been extensively developed for the case of closely spaced Stark components of paramagnetic ion levels in insulators.³⁰ In adapting it to the case of the (A^0, X) complex, we assume that the 1S level fine structure consists of the two observed components. Then, the lowest-energy component will have the following linewidth dependence on temperature (one-phonon processes):

$$\delta(T) = A + \frac{B}{\exp(\Delta E/kT) - 1}. \quad (2)$$

A is the residual (inhomogeneous) linewidth at $T=0$, and B is a coefficient which incorporates the exciton-acoustic-phonon interaction strength and phonon density of states. ΔE is energy separation between the two

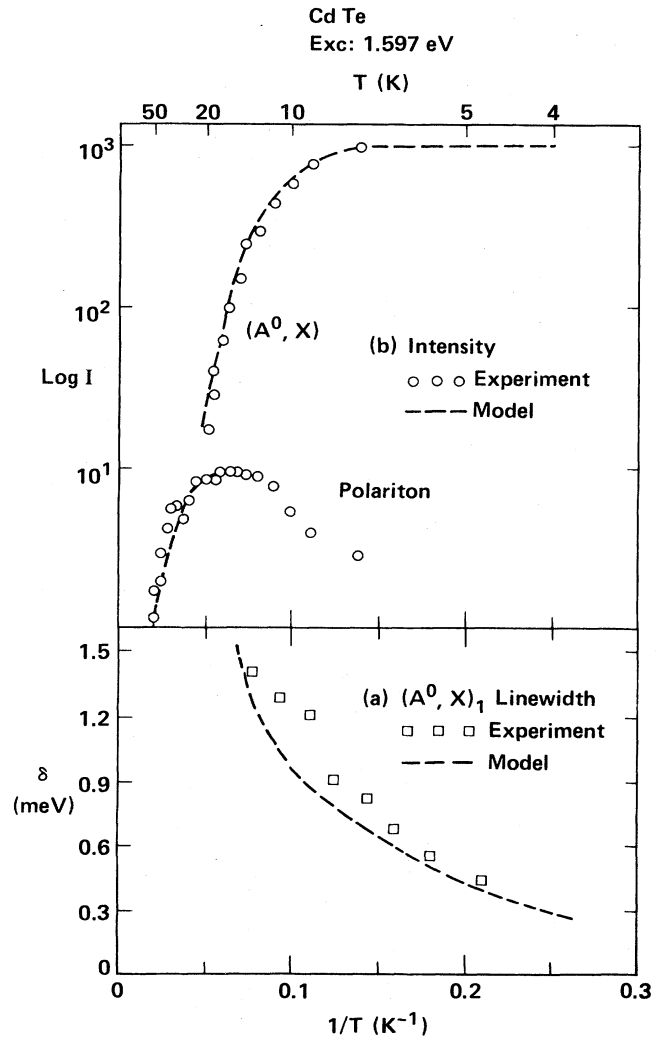


FIG. 4. (a) Temperature dependence of the lowest (A^0, X) 1S component linewidth. (b) Temperature dependence of the integrated luminescence intensity of the polariton and the (A^0, X) bands in CdTe. Dashed lines are obtained using the models described in text.

(A^0, X) 1S components. This separation is itself temperature dependent, varying from 1 meV at 4.2 K to 1.4 meV at 14 K. The solid curve in Fig. 4(a) is obtained using Eq. (2) with $A=0.1$ meV, $B=3$ meV, and the measured values of ΔE . The deviation of this curve from the observed linewidths may be due to the omission of the third (A^0, X) $J = \frac{1}{2}$. The pronounced dependence of the (A^0, X) 1S linewidths on temperature, as compared to the weak dependence of the (D^0, X) lines, is a consequence of the stronger (A^0, X) interaction with acoustic phonons. Since the same relative interaction strength is found for LO phonons, we conclude that the strongest interaction is with piezoelectric phonons (rather than by the deformational potential). It is interesting to note that the (residual) inhomogeneous broadening of the $(A^0, X)_1$ line is smaller than that of the three (D^0, X) components. It thus appears that the acceptor-bound excitons are less affected by

random, static electric field than the donor-bound excitons. The situation is reversed for the case of phonon-induced broadening and, as we shall see in Sec. III B, for alloy broadening.

The integrated luminescence intensity of the polariton band, the shallow S band, and the (A^0, X) lines has been measured as a function of temperature. In these experiments, excitation was at 1.597 eV, slightly above the 1S polariton threshold, and the excitation intensity was maintained constant. Figure 4(b) shows the logarithm of the intensity plotted versus inverse temperatures for the polariton band and the (A^0, X) lines. The temperature dependence of the S band is virtually identical to that of the polariton band.

As observed in other semiconductors,³¹ the temperature dependence of the (A^0, X) luminescence intensity can be fitted by the expression

$$I_A(T) = \frac{I_0}{1 + C_A \exp(-E_A/kT) + C_f \exp(-E_f/kT)}. \quad (3)$$

The parameters used in fitting the data are $C_A = 300 \pm 100$, $C_f = (5 \pm 2) \times 10^4$, $E_A = 6 \pm 1$, and $E_f = 14 \pm 1$ meV. For the polariton band in the temperature range $15 < T \leq 80$ K, the data can be fitted by the expression

$$I_{\text{pol}}(T) = \frac{I_0}{1 + C_{\text{pf}} \exp(-E_{\text{pf}}/kT)}, \quad (4)$$

with the parameters $C_{\text{pf}} = 100 \pm 50$ meV and $E_{\text{pf}} = 12 \pm 1$ meV. A comparison of the fitted activation energies with those determined spectroscopically allows identification of the nonradiative exciton recombination processes. The value obtained for E_{pf} is close to the known exciton binding energy, $E_x = 10$ meV.³² Thus, the main nonradiative recombination process of the polaritons is their dissociation. The same process can be identified for the (A^0, X) excitons, corresponding to the activation energy of $E_f = 14$ meV. The spectroscopically determined energy is 15.7 meV. The preexponential factor for exciton dissociation is about 2 orders of magnitude larger for (A^0, X) than it is for polaritons. A possible explanation is the following: A quasiequilibrium state is maintained between the polaritons and the free carriers. On the other hand, if excitons dissociating at neutral acceptors cannot be captured by other acceptors (as other recombination or capture paths are more efficient), a quasiequilibrium state will not be established and the rate of this process will be higher than for polaritons.

The process with $E_A = 6$ meV observed for (A^0, X) can be identified as an exciton thermalization into the free-exciton (polariton) band, leaving a neutral acceptor behind. The concurrent increase in polariton luminescence intensity [Fig. 4(b)], agrees well with the proposed process.

3. Resonant Raman scattering

Raman scattering by LO phonons is observed throughout the band-edge spectral region. Figure 5 shows the Raman scattering cross section (in arbitrary units) measured at 1.7 K. No resonant enhancement was ob-

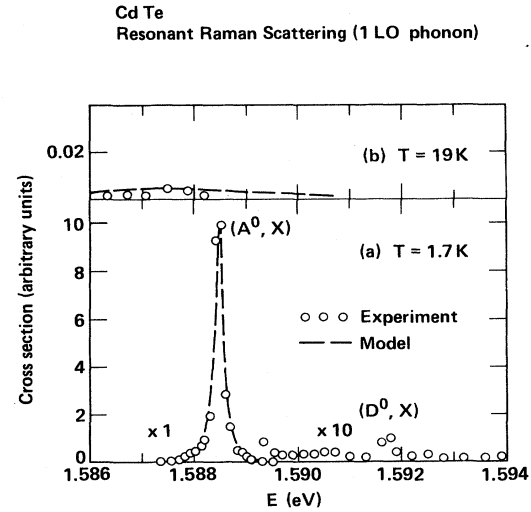


FIG. 5. Cross sections of resonant Raman scattering by LO phonon in CdTe. Dashed curves are calculated assuming a Lorentzian line shape with FWHM of 0.1 meV at 1.7 K and 4.5 meV at 19 K.

served for excitation near the 1S polariton (excitation energy above 1.595 eV). Nakamura and Weisbuch²¹ reported strong enhancement in this spectral region. A possible explanation for this discrepancy between the two observations may be the shorter polariton lifetime in the less pure crystals used in the present study.³³ A strong resonant enhancement is observed at the lowest $(A^0, X)_1$ level (by a factor of 200 above that of the adjacent spectral regions). No enhancement is observed at the upper $(A^0, X)_2$ level. For temperatures below 5 K the Raman line could be distinguished from the (A^0, X) -LO-phonon sideband for excitation as close as 0.1 meV to the peak of the $(A^0, X)_1$ line. This is a consequence of the sharpness of both the $(A^0, X)_1$ line and its phonon replica. In the temperature range of 5–17 K, the Raman line cannot be observed because of the broad (A^0, X) -LO luminescence but it reappears at higher temperatures [Fig. 5(b)] as the luminescence intensity is greatly reduced.

The shape of the cross-section spectrum can be well fitted by the equation¹³

$$I(E) = \frac{C\gamma}{(E - E_0)^2 + \gamma^2}, \quad (5)$$

where E_0 is the $(A_0, X)_1$ energy, C is a proportionality factor, and $\gamma(T)$ is the exciton damping factor. At $T = 1.7$ K, the data can be fitted with $\gamma = 0.1$ meV, as shown by the dashed curve in Fig. 5(a).

As we do not have cross-section spectra for all temperatures, the dependence of γ on temperature cannot be determined. The 19-K data [Fig. 5(b)] can be compared with the calculated cross section using $\gamma = 4 \pm 1$ meV [obtained from Eq. (2)]. Note the shift in the (weak) resonance towards lower energies, following the shift in (A^0, X) line position (cf. Fig. 2). The decrease in intensity due to line broadening explains the lack of enhanced resonance

for the $(A^0, X)_2$ level, which has a width of 0.4 meV even at 1.7 K.

Finally, we note the very weak resonance near the (D^0, X) line. This is another manifestation of the weak interaction of the donor-bound exciton with LO phonons.

The results obtained here for bound-exciton enhancement of Raman scattering can be compared with the only other reported study on CdS by Damen and Shah.³⁴ In that case, a strong resonance was observed near both (A^0, X) and (D^0, X) lines, with linewidth 10 times larger than that observed here for CdTe. (The luminescence linewidths are comparable.) Possibly the large linewidth was due to the fact that a high-intensity pulsed dye laser was used in the study of CdS. The presence of a high density of excitons (and free carriers) could contribute to a larger exciton damping.

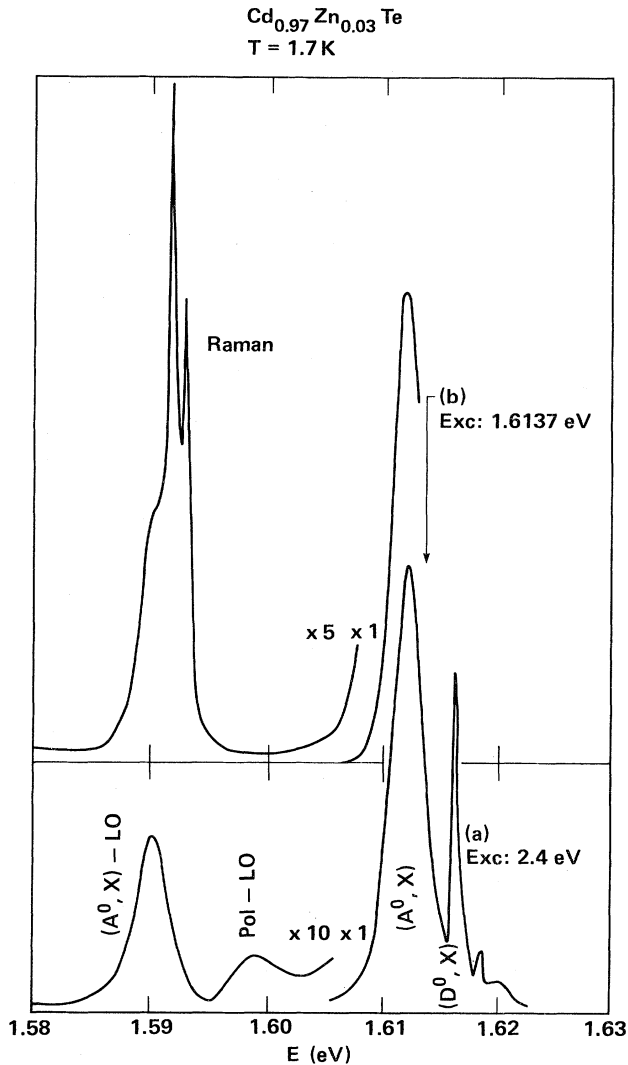


FIG. 6. Photoluminescence and RRS of $\text{Cd}_{0.97}\text{Zn}_{0.03}\text{Te}$. (a) Excitation deep in the conduction band and (b) selective excitation into the (A^0, X) band. Two sharp lines near 1.592 eV are the two LO-phonon Raman lines resonantly enhanced at the (A^0, X) band.

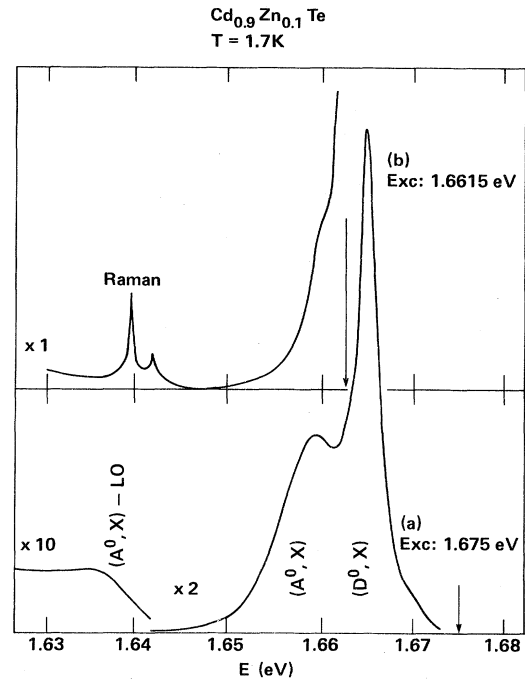


FIG. 7. Same as Fig. 6 but for $\text{Cd}_{0.9}\text{Zn}_{0.1}\text{Te}$.

B. $\text{Cd}_x\text{Zn}_{1-x}\text{Te}$

1. Exciton levels

In the alloy semiconductors the (D^0, X) and (A^0, X) levels broaden. Figures 6(a) and 7(a) show the luminescence spectra obtained under above-gap excitation at $T=1.7$ K for $x=0.03$ and 0.1 , respectively. The broadening results from random potential fluctuations experienced by the bound exciton.¹ The line shapes of both (D^0, X) and (A^0, X) are well fitted by Gaussians whose FWHM are given in Table II. For $x=0.03$, the internal (fine) structure of the (D^0, X) exciton can still be resolved. According to the model proposed by Suslina *et al.*,⁵ the linewidth dependence on the composition parameter x is

$$\delta(x) = \left[\ln 2 \frac{x(1-x)}{\pi N(x)} \right]^{1/2} \frac{dE}{dx} a_B^{-3/2}, \quad (6)$$

where N is the number of lattice sites per unit volume and (dE/dx) is the slope of bound-exciton energy with respect to x . This slope is equal to (dE_{gap}/dx) , as the binding energy of either (D^0, X) or (A^0, X) varies only slightly for

TABLE II. FWHM of (D^0, X) and (A^0, X) lines at $T=1.7$ K (in meV).

	(D^0, X)			(A^0, X)	
	1	2	3	1	2
CdTe	0.28	0.25	0.20	0.1	0.4
$\text{Cd}_{0.97}\text{Zn}_{0.03}\text{Te}$	0.75	0.70	0.60		3.4
$\text{Cd}_{0.9}\text{Zn}_{0.1}\text{Te}$		2.2			8.5

$x \leq 0.1$. a_B^3 is a measure of the volume occupied by the bound exciton. Comparing the linewidths of (D^0, X) and (A^0, X) for both $x=0.03$ and 0.1 , we obtain

$$\frac{\delta_A}{\delta_D} = \left[\frac{a_D}{a_A} \right]^{3/2} \approx 4.$$

Thus, $a_D/a_A \sim 2.5$, indicating that the (D^0, X) complex extends over a much larger volume than the (A^0, X) complex. This result is consistent with the ratio of effective-mass Bohr radii of the neutral donor and acceptor ($a_{D^0}/a_{A^0} \sim 4$).

In addition to the bound-exciton bands, the free-exciton band is clearly observed in $\text{Cd}_{0.97}\text{Zn}_{0.03}\text{Te}$. This band is analogous to the polariton band in CdTe and, indeed, has a similar LO-phonon sideband. A close comparison between the phonon sidebands of these two crystals indicates that the free-exciton band of the mixed crystal has a sharp low-energy cutoff (< 1 meV) and does not show a tail of states due to disorder. Such a tail has been observed in $\text{CdS}_{0.995}\text{Se}_{0.005}$.⁹ However, the effective-mass Bohr radius of the exciton in CdTe is twice as large as that in CdS. Potential fluctuations are thus better averaged out in $\text{Cd}_x\text{Zn}_{1-x}\text{Te}$ than in $\text{CdS}_x\text{Se}_{1-x}$.

In $\text{Cd}_{0.9}\text{Zn}_{0.1}\text{Te}$, a weak shoulder is observed on the high-energy side of (D^0, X) at 1.668 eV. This band could be due to intrinsic excitons. However, based on the existing data, this assignment is tentative only.

A series of selectively excited luminescence spectra reveal line narrowing and spectral diffusion within the (A^0, X) band. Figures 6(b) and 7(b) show two examples. The sharp lines at the LO-phonon region are Raman lines and will be discussed in Sec. III B 2. The possibility that an acoustic-phonon sideband (associated with the selectively excited sites) is observed at 1.612 eV [Fig. 6(b)] can be ruled out for the following reasons: (a) No acoustic-phonon sideband is observed associated with the strong (A^0, X) line in CdTe, and (b) in both $\text{Cd}_{0.97}\text{Zn}_{0.03}\text{Te}$ and $\text{Cd}_{0.9}\text{Zn}_{0.1}\text{Te}$, the observed spectral diffusion does not show a constant Stokes shift for excitation within the (A^0, X) band.

We have calculated the expected spectral line shape assuming transfer within the (A^0, X) band using the model of Ref. 10. We found that for effective transfer to occur, its rate must be greater than the radiative recombination rate. This requires two conditions which are not met in the present case: (a) a strong exciton-acoustic-phonon interaction (such as in $\text{CdS}_x\text{Se}_{1-x}$ crystals), and (b) a large overlap between exciton-binding sites. The latter is not expected to happen as the concentration of neutral acceptors is small. (Assuming a random distribution of 10^{16} acceptors/cm³, the average separation between acceptors is about 100 lattice sites. The exciton Bohr radius is only 10 lattice sites.) We thus conclude that the observed spectral diffusion within the (A^0, X) band must occur via an intermediary impurity. The data suggest that the impurities giving rise to the *S*-band luminescence fulfill this role. Excitation spectra of various parts of the (A^0, X) band in $\text{Cd}_{0.97}\text{Zn}_{0.03}\text{Te}$ are similar to those of CdTe [Fig. 3(a)]. They show that the low-energy tail of the *S* band overlaps

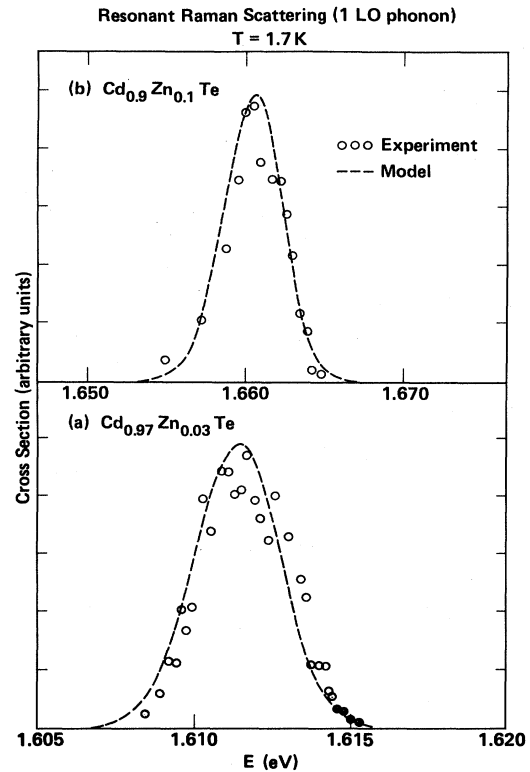


FIG. 8. Cross section of resonant Raman scattering by LO phonon in (a) $\text{Cd}_{0.97}\text{Zn}_{0.03}\text{Te}$ and (b) $\text{Cd}_{0.9}\text{Zn}_{0.1}\text{Te}$ at 1.7 K. Solid curves are calculated assuming a Gaussian line shape with parameters given in text.

with the (A^0, X) band. Since at low temperatures the *S*-band luminescence is much weaker than that of the (A^0, X) band, transfer from the former to the latter is very efficient. The concentration of impurities contributing to the *S* band must be very high, as its luminescence is as strong as the free-exciton luminescence at elevated temperatures.

2. Raman scattering

Raman scattering by LO-phonon modes is observed in $\text{Cd}_x\text{Zn}_{1-x}\text{Te}$ ($x \geq 0.9$) under excitation in the free- and bound-exciton spectral region. Examples are shown in Figs. 6(b) and 7(b). This alloy semiconductor is known to be a two-vibrational-mode system,^{35,16} and two LO phonons are clearly resolved even for $x=0.98$ at 1.7 K. The lower-energy LO phonon has virtually the same energy as the LO phonon in CdTe (21 meV). Upon increasing the Zn content, the intensity of this mode decreases with respect to that of the higher-energy LO mode. The energy of the latter increases from 22.2 meV for $x=0.97$ to 22.7 meV for $x=0.9$. This behavior is consistent with associating the 21-meV mode with vibrations of the (heavier) CdTe sublattice and the other mode with the ZnTe sublattice. (It should be noticed that the associated TO-phonon Raman lines are very weak, but observable with energies of 18.3 and 19.5 meV in $\text{Cd}_{0.97}\text{Zn}_{0.03}\text{Te}$.)

As in the case of CdTe, strong resonance enhancement

of the LO-phonon scattering is observed only in the (A^0, X) spectral region. The scattering cross-section dependence on energy is shown in Fig. 8 for both $\text{Cd}_{0.97}\text{Zn}_{0.03}\text{Te}$ and $\text{Cd}_{0.9}\text{Zn}_{0.1}\text{Te}$, normalized with respect to the peak intensity. The energy of the peak scattering in both crystals coincides with that of the peak luminescence. Assuming that only the (A^0, X) band contributes to the RRS, the shape of the cross-section curve is given by the following expression¹³:

$$\sigma(E) = C \int_{(A^0, X)} \frac{\gamma(E_i, T) P(E_i) dE_i}{(E - E_i)^2 + \gamma^2(E_i, T)}. \quad (7)$$

E is the excitation (laser) energy, and $P(E_i)$ is the probability of finding an intermediate state at energy E_i . $P(E_i)$ should, in principle, be identical with the (Gaussian) line shape of the (A^0, X) band in the alloy semiconductor. $\gamma(E_i, T)$ is the bound-exciton damping factor which depends on both exciton energy and crystal temperature (see below). C contains all the proportionality factors and also implies integration over final states (which yields the same result for each intermediate state). In fitting the experimentally observed cross-section curves at 1.7 K, the damping factor is taken as the (A^0, X) linewidth of CdTe at this temperature (0.1 meV). The results of the fit using Eq. (7) and a Gaussian form for $P(E_i)$ are shown as dashed lines in Figs. 8(a) and 8(b). For $\text{Cd}_{0.97}\text{Zn}_{0.03}\text{Te}$, the FWHM is 3.1 ± 0.1 meV as compared with 3.4 ± 0.1 meV obtained for the luminescence curve. For $\text{Cd}_{0.9}\text{Zn}_{0.1}\text{Te}$, the Raman FWHM is 4.3 ± 0.2 meV, while that of the luminescence curve is 8.5 ± 0.2 meV. The discrepancy between these linewidths suggests that the wings of the (A^0, X) band contain states with a different electronic structure from that of the (A^0, X) bound exciton (at least as far as the scattering efficiency is concerned).

As the temperature is increased, the Raman intensity drops. Figure 8 shows the observed Raman-intensity dependence on temperature, for several excitation energies within the (A^0, X) band of $\text{Cd}_{0.97}\text{Zn}_{0.03}\text{Te}$. Also shown is the integrated luminescence intensity dependence on temperature for the (A^0, X) band. The latter can be fitted using Eq. (3) with the parameters $C_A = 500 \pm 200$, $C_f = (10 \pm 5) \times 10^4$, and $E_f = 14 \pm 2$ meV. As in the case of CdTe, the two nonradiative recombination processes are exciton dissociation (activation energy of 14 ± 2 meV) and exciton thermalization into the free-exciton band. In fitting the data, the activation energy for exciton thermalization [E_A of Eq. (3)] was taken as the energy separation of each section of the (A^0, X) band from the bottom of the free-exciton band.

As can be seen from Fig. 9, the temperature dependence of the Raman lines is different from that of the integrated luminescence intensity, and is dependent on the excitation energy. This observation is important evidence for identifying the pair of sharp LO-phonon lines as Raman scattering rather than luminescence. The temperature dependence of the Raman lines comes from that of the damping factor $\gamma(E_i, T)$ in Eq. (7). In principle, the same nonradiative recombination processes governing exciton luminescence should contribute to exciton damping, and we can write

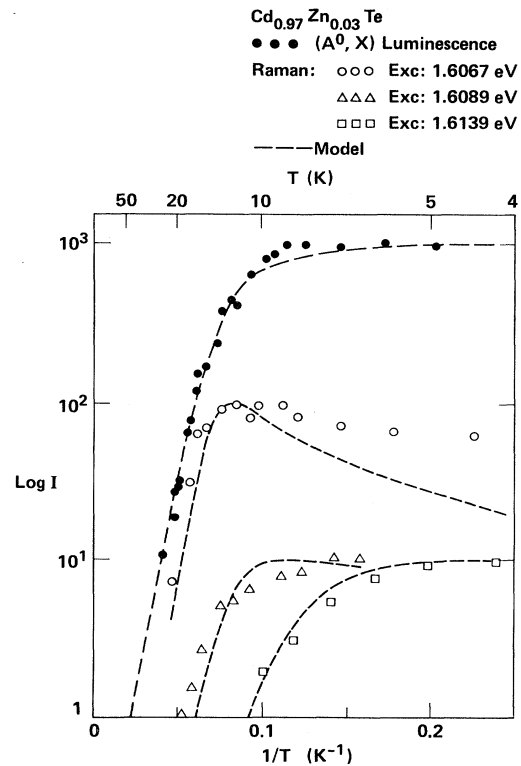


FIG. 9. Temperature dependence of the integrated luminescence intensity of the (A^0, X) band and LO-phonon Raman lines excited at various points within this band. Dashed curves are calculated using exciton damping processes as explained in text.

$$\gamma(E_i, T) = A + \frac{B}{\exp(\Delta E/kT) - 1} + C'_A \exp(-\Delta E_i/kT) + C'_f \exp(-E_f/kT). \quad (8)$$

The first two terms are the homogeneous (A^0, X) linewidth [Eq. (2)]. The parameters C'_A and C'_f are the damping factors (for $T \rightarrow \infty$) due to exciton thermalization and dissociation, respectively. C'_A may depend on exciton energy if thermalization is through intermediate states (such as the shallow S band). This can be probed by the RRS since the spectral regions contributing most to the scattering are those adjacent to the excitation energy. [It must be remembered that the luminescence dependence on temperature yielded average values for the preexponential parameters, as the intensity was integrated over the whole (A^0, X) band.] In fitting all the Raman curves of Fig. 8, we used the same homogeneous line parameters as for CdTe ($A=0.1$, $B=3.0$ meV, and for ΔE a constant value of 1.1 meV). The activation energies are the same as used in fitting the luminescence-intensity dependence on temperature; $E = 14 \pm 2$ meV for exciton dissociation, and $\Delta E_i = E_x - E_i$, where E_x is the energy of the free exciton. For the exciton dissociation damping factor we obtain $C'_f = (10 \pm 5) \times 10^5$ meV throughout the band. This process is the predominant contributor to exciton damping for $T > 10$ K. For the exciton thermalization pre-

exponential factor we obtain $C'_A = (3 \pm 1) \times 10^2$ meV for $E_i \leq 1.612$ eV. However, for excitation at the top of the (A^0, X) ($E_i \sim 1.614$ eV), $C'_A = 10^5$ meV. This large value indicates that excitons in this part of the band thermalize faster with the free-exciton band than those deeper in the (A^0, X) band.

The fit of this model to the Raman data is not as good as that of the luminescence data and may expose the oversimplified approach in describing damping mechanisms. Also, part of the Raman signal may be due to luminescence. A time-resolved spectroscopy study may shed light on this problem.

IV. SUMMARY

The spectroscopic properties of (A^0, X) and (D^0, X) excitons (1S state) in CdTe and $\text{Cd}_x\text{Zn}_{1-x}\text{Te}$ ($x \geq 0.9$) have been studied by selectively excited luminescence and by resonant Raman scattering of LO phonons. The large disparity between the (D^0, X) and (A^0, X) exciton-acoustic-phonon interaction manifests itself in the different dependence of the exciton linewidth on temperature in CdTe. The more strongly interacting (A^0, X) exciton levels have Lorentzian line shapes strongly dependent on temperature, while the weakly interacting (D^0, X) exciton levels are Gaussian with a very small contribution from phonon broadening. Since the (A^0, X) exciton interacts strongly with the LO phonons, it shows a very pronounced RRS. The analogy between the interaction strength with LO and acoustic phonons indicates that the coupling must be due mainly to the piezoelectric interaction (and not to the deformation potential). There are no detailed models that can account for the different interaction strength between (A^0, X) and piezoelectric phonons and that of (D^0, X) . However, Hopfield's model for a single bound particle³⁶ indicates that the interaction is stronger for more localized particles. As deduced from the linewidths of the (A^0, X) and (D^0, X) bands in the alloys, the former is more localized. Although these are three particle systems, this finding is consistent with the relative strengths of phonon interactions.

The (A^0, X) and (D^0, X) also couple differently to static potential fluctuations. In CdTe, the (D^0, X) lines are Gaussian and broader than the $(A^0, X)_1$ line at 1.7 K. The commonly suggested line-broadening mechanism at very low temperatures is coupling to random, static electric fields. The data suggest that the (A^0, X) level couples less to these fields than the (D^0, X) levels do. The situation is different when alloying with ZnTe is introduced. The (A^0, X) lines are much more sensitive to alloying, and the linewidth increases at a rate fourfold greater than that of

the (D^0, X) levels. As was recently found for $\text{Ga}_x\text{In}_{1-x}\text{As}$,³⁷ alloying causes changes in both bond lengths and bond angles. As the acceptor levels consist mainly of p orbitals, while the donor of s orbitals, the former is expected to be more sensitive to alloying than the latter, as indeed is observed.

We have studied the temperature dependence of (A^0, X) luminescence and LO-phonon RRS and tried to treat it by a unified model of bound-exciton dynamics (i.e., temperature-dependent relaxation processes). The luminescence data could be well explained by two nonradiative recombination processes, exciton thermalization into the free-exciton band and exciton dissociation. By using the same processes, the fit to the temperature dependence of the RRS is not as good as that of the luminescence intensity. Clearly the simple model of exciton damping does not fully explain the RRS data. More work, in particular, on time-resolved spectroscopy (with picosecond resolution) is required.

It is interesting to note that the spectral diffusion within the (A^0, X) band, observed in the alloy semiconductors, is not due to direct transfer between (A^0, X) sites, but rather to transfer through an intermediary, shallow bound-exciton band (designated S in this study). The tail of the S band overlaps the (A^0, X) band, and judging from its strong intensity at elevated temperature it is due to some centers with a high concentration. The available data is insufficient to determine its origin.

Finally we can compare the results obtained here with similar experiments done on $\text{CdS}_x\text{Se}_{1-x}$.^{9,10} In the latter, the excitons are localized by intrinsic potential fluctuations¹¹ rather than by impurities as is the case in $\text{Cd}_x\text{Zn}_{1-x}\text{Te}$. This is not due to a higher impurity content in $\text{Cd}_x\text{Zn}_{1-x}\text{Te}$. The relative intensity of LO-phonon sidebands of the polariton bound-exciton bands are similar in high-purity CdS and CdTe crystals. It must arise from the difference in exciton Bohr radii, 28 and 70 Å, respectively.³² Short-range, intrinsic potential fluctuations are thus averaged out in $\text{Cd}_x\text{Zn}_{1-x}\text{Te}$ to a much greater extent than in $\text{CdS}_x\text{Se}_{1-x}$. The sharp LO-phonon lines in $\text{Cd}_x\text{Zn}_{1-x}\text{Te}$ have been identified as resonantly enhanced Raman scattering. Time-resolved spectroscopy on the analogous lines in $\text{CdS}_x\text{Se}_{1-x}$,¹¹ has shown that in this system they are actually resonant luminescence. The bands at which these lines are (selectively) excited are different for $\text{CdS}_x\text{Se}_{1-x}$ and $\text{Cd}_x\text{Zn}_{1-x}\text{Te}$. It would thus be of interest to perform similar experiments on $\text{Cd}_x\text{Zn}_{1-x}\text{Te}$ in order to determine the relative contribution (if any) of luminescence to the sharp LO-phonon lines.

*On sabbatical leave from the Department of Physics and Solid State Institute, Technion, Haifa 32000, Israel.

¹S. D. Baranovskii and A. L. Efros, *Fiz. Tekh. Poluprovodn.* **12**, 2233 (1978) [*Sov. Phys.—Semicond.* **12**, 1328 (1978)].

²R. J. Nelson, in *Excitons*, Vol. 2 of *Modern Problems in Condensed Matter Sciences*, edited by E. I. Rashba and M. D. Sturge (North-Holland, Amsterdam, 1982), p. 319.

³A. N. Pikhtin *Fiz. Tekh. Poluprovodn.* **11**, 425 (1977) [*Sov. Phys.—Semicond.* **11**, 245 (1977)].

⁴D. J. Wolford, W. Y. Hsu, J. D. Dow, and B. G. Streetman, *J. Lumin.* **18&19**, 863 (1979).

⁵L. G. Suslina, A. G. Plyukhin, O. Geode, and D. Hennig, *Phys. Status Solidi B* **94**, K185 (1979).

⁶J. A. Kash, J. H. Collet, D. J. Wolford, and J. Thompson,

- Phys. Rev. B 27, 2294 (1983).
- ⁷R. Stegmann, B. Kloth, and G. Oelgart, Phys. Status Solidi A 70, 423 (1982).
- ⁸M. D. Sturge, E. Cohen, and R. A. Logan, Phys. Rev. B 27, 2362 (1983).
- ⁹S. Permogorov, R. Reznitskii, S. Verbin, G. O. Müller, P. Flögel, and M. Nikeforova, Phys. Status Solidi B 113, 589 (1982).
- ¹⁰E. Cohen and M. D. Sturge, Phys. Rev. B 25, 3828 (1982).
- ¹¹J. A. Kash, A. Ron, and E. Cohen (unpublished).
- ¹²J. H. Collet, J. A. Kash, D. J. Wolford, and J. Thomson, J. Phys. C 16, 1283 (1983).
- ¹³R. M. Martin and L. M. Falicov, in *Light Scattering in Solids*, Vol. 8 of *Topics in Applied Physics*, edited by M. Cardona (Springer, Berlin, 1975).
- ¹⁴E. S. Koteles, in *Excitons*, Vol. 2 of *Modern Problems in Condensed Matter Sciences*, Ref. 2.
- ¹⁵A. Nakamura and C. Weisbuch, Solid State Commun. 32, 301 (1979).
- ¹⁶A. S. Barker and A. J. Sievers, Rev. Mod. Phys. 47, Suppl. No. 2, S1 (1975).
- ¹⁷A. A. Klochikhin, A. G. Plyukhin, L. G. Suslina, and E. B. Shadrin, Fiz. Tverd. Tela (Leningrad) 18, 1909 (1976) [Sov. Phys.—Solid State 18, 1112 (1976)].
- ¹⁸A. Fujii, H. Stolz and W. von der Osten, J. Phys. C 16, 1713 (1983).
- ¹⁹Details of the crystal growing and electrical characterization are given by A. Muranevich, M. Roitberg, and E. Finkman, J. Cryst. Growth (to be published).
- ²⁰P. Hiesinger, S. Suga, F. Willmann, and W. Dreybrodt, Phys. Status Solidi B 67, 641 (1975).
- ²¹A. Nakamura and C. Weisbuch, Solid State Electron. 21, 1331 (1978).
- ²²K. Cho, W. Dreybrodt, P. Hiesinger, S. Suga, and F. Willmann, in *Proceedings of the 12th International Conference on the Physics of Semiconductors*, edited by M. H. Pilkuhn (Teubner, Stuttgart, 1975), p. 945.
- ²³R. G. Ulbrich, N. V. Hiew, and C. Weisbuch, Phys. Rev. Lett. 46, 53 (1981).
- ²⁴A. M. White, J. Phys. C 6, 1971 (1973).
- ²⁵D. C. Herbert, J. Phys. C 10, 3327 (1977).
- ²⁶A. M. White, P. J. Dean, and B. Day, J. Phys. C 7, 1400 (1974).
- ²⁷E. Molva and L. S. Dang, Phys. Rev. B 27, 6222 (1983).
- ²⁸D. M. Larsen, Phys. Rev. B 13, 1681 (1976).
- ²⁹R. L. Greene, Phys. Rev. B 27, 6512 (1983).
- ³⁰W. M. Yen, W. C. Scott, and A. L. Schawlow, Phys. Rev. 136, A271 (1964).
- ³¹D. Bimberg, M. Sondergeld, and E. Grobe, Phys. Rev. B 4, 3451 (1971).
- ³²B. Segall and D. T. F. Marple, in *Physics and Chemistry of II-VI Compounds*, edited by M. Aven and J. S. Prener (North-Holland, Amsterdam, 1967), p. 335.
- ³³S. Borenstain and E. Cohen (unpublished).
- ³⁴T. C. Daman and J. Shah, Phys. Rev. Lett. 27, 1506 (1971).
- ³⁵H. Harada and S. Narita, J. Phys. Soc. Jpn. 30, 1628 (1971).
- ³⁶J. J. Hopfield, J. Phys. Chem. Solids 10, 110 (1959).
- ³⁷J. C. Mikkelsen and J. B. Boyce, Phys. Rev. Lett. 49, 1412 (1982).